IOSR Journal of Applied Physics (IOSR-JAP)
e-ISSN: 2278-4861.Volume 10, Issue 6 Ver. II (Nov. – Dec. 2018), 58-63
www.iosrjournals.org

Crystallographic and Magnetic Properties with Increasing Co^{2+} In $Cu_{0.60-X}co_xzn_{0.40}Fe_2O_4$ $(0 \leq X \leq 0.5)$ Nanoferrites

D. D. Birajdar[1*]
[1]B.S.S. Arts,Science and Commerce college Makani, Osmanabad (M.S.), India
Corresponding Author: D. D. Birajdar

Abstract: *Nanoparticles of $Cu_{0.60-x}Co_xZn_{0.40}Fe_2O_4$ $(0 \leq x \leq 0.5)$ are prepared by sol-gel auto combustion method. Copper nitrate, cobalt nitrate, zinc nitrate, ferric nitrate and citric acid used as the starting materials. Cations redistribution takes place for $x > 0.3$. Saturation magnetization increases from 52.99 to 79.62 emu/gm $(x \leq 0.3)$. For $x > 0.3$ Ms decreases suggesting that significant canting exists at B site. However, coercivity, magnetocrystalline anisotropy and remanant magnetization increases with the Co^{2+} substitution.*

PACS No. *75.50.Gg, 73.63.Bd, 91.60.Pn*
Keywords: *Sol-gel synthesis, cation distribution, redistribution, M_S, H_C, Mr.*

Date of Submission: 04-01-2019 Date of acceptance: 21-01-2019

I. Introduction

Copper spinel ferrite is an inverse ferromagnetic spinel. It is considered that the $CuFe_2O_4$ is a ferrite of Cu^{2+}. The cation distribution in this copper ferrite can be presented by the formula $(Cu^{2+}{}_x+Fe^{3+}{}_{1-x})^A$ $[Cu^{2+}{}_{1-x}+Fe^{3+}{}_{1+x}]^BO_4$. The parameter of inversion is $(0 \leq x \leq 0.5)$ When the spinel is normal, Cu^{2+} cations migrate from octahedral (B-sublattice) to tetrahedral places (A-sublattice) Yokoyama et al. [2] observed changes in the crystal structure of nanosized $CuFe_2O_4$ powders obtained by coprecipitation and subsequently annealed. According to other authors [3] a = 8.24, c = 8.68, but c/a is again 1.05. According to some authors, the transition from tetragonal to cubic structure has to do with changes in the oxygen content in the lattice, i.e. with formation of observable quantities of Cu^+. Kester et al. [4] proved that in the case of the reduction reaction for quenched samples of $CuFe_2O_4$, the mechanism involves the formation of Cu^+. The rate of reduction, i.e. the Cu^+ cation fraction in the B-sublattice strongly depends on the technologies of synthesis and the subsequent temperature treatment. Magnetization behavior and magnetic ordering of Cu-Zn ferrites hav studied by many workers [5-7] reported increase in magnetic properties around $Cu_{0.60-x}Co_xZn_{0.40}Fe_2O_4$ composition. Magnetic ions substitution in simple and mixed ferrites has received a great deal over the past years [8, 9]. The presences of these ions in spinel ferrites alter their structural, magnetic and electrical properties. Further Co ferrite shows the good magnetostrictive properties, magnetocrystalline anisotropy, high coercivity and moderate saturation magnetization among all the ferrite family [10]. Therefore, by keeping this view along with $Cu_{0.60-x}Co_xZn_{0.40}Fe_2O_4$ composition in our mind we have proposed the studies on structural analysis, cation distribution and magnetic properties of nano-size $Cu_{0.60-x}Co_xZn_{0.40}Fe_2O_4$ $(0 \leq x \leq 0.5)$ by sol-gel method.

II. Experimental

2.1 Preparation method:

In order to achieve a complete reaction within short time and at the lowest possible temperatures, composition of component cations at an atomic scale is necessary. Sol-gel auto-combustion method is a novel method of preparing nano-materials [11]. The precursor is not calcined at high temperature, thus it can save energy and avoid agglomeration during the calcination at high temperature. The as prepared powder then annealed at 600 ^{0}C for 4 h.

2.2 Structural and magnetic characterization:

The dried gels were characterized via thermogravimetric (TGA) and differential thermal analysis (DTA) at a heating rate of 10^0C/min in air atmosphere. The scanning step was 2^0/min and scanning range was 20-80°.

III. Results and discussion

3.1 Structural properties

The experimental observation showed that the nitrate–citrate gels with all three molar ratios of metal nitrates to citric acid exhibited self-propagating combustion behavior. The autocatalytic nature of the combustion process of gels has been studied by thermal analysis (DTA and TGA) of the dried gels. The TGA of the mid sample x = 0.3 decomposing in air atmosphere in the temperature range 20 to 700^{0}C with a heating rate of 10 ^{0}C/min is shown in Fig. 1.

fig.1

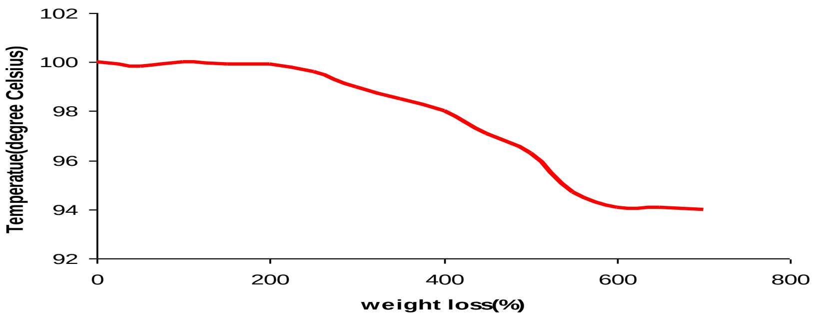

The observed weight loss below 100^{0}C of x = 0.3 sample for Co is attributed to the loss of physically or chemically absorbed OH groups. The end-products after decomposition were identified as single spinel phase Cu–Co–Zn ferrite, from the analysis of their recorded XRD patterns (Fig. 2).

Fig.2

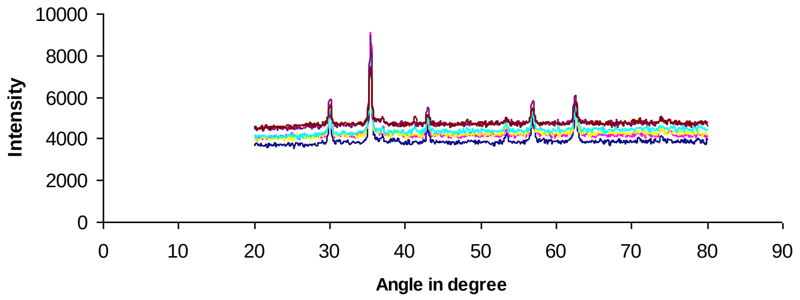

This proves the simultaneous completion of decomposition process of oxalate complex and ferritization.The variation of lattice constant with composition x is shown in Fig3.

Fig.3

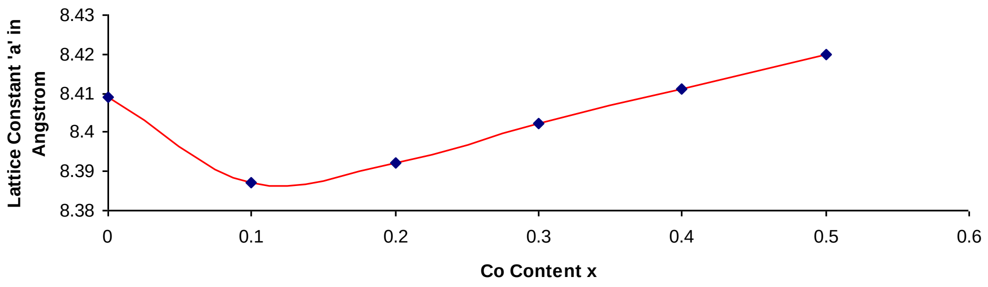

It is clear from Fig. 3 that lattice constant decreases with increase in x for x = 0.1. For x > 0.1 lattice constant increases with composition x. Generally, in a solid solution series linear increase or decrease of lattice constant within the miscibility range with composition is observed [12]. This may results into initial decrease in lattice constant up to x = 0.1 beyond which it increases. This nonlinear behavior of lattice constant suggests that the ferrite system is not completely normal or inverse. In the present series, $Cu_{0.60\text{-}x}Co_xZn_{0.40}Fe_2O_4$ ($0 \leq x \leq 0.5$)

smaller Cu^{2+} (0.72Å) ions are replaced by larger Co^{2+} (0.745Å) [13]. Since each primitive unit cell of the spinel structure contains eight molecules, the X-ray density, d_X' was determined according to the following relation [14] and are shown in Fig.4.

Fig. 4

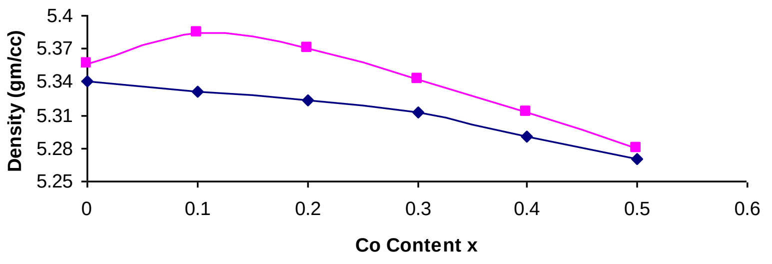

$$d_x(Ferrite) = \frac{8M}{N \times a^3}$$

where M is molecular weight of the particular ferrite, N is the Avogadro's number and a^3 is the volume of the cubic unit cell. It is also evident from the crystallite size of 25-34 nm for all samples estimated from the most intense peak (311) using the Scherrer equation, $D_{hkl} = 0.9\lambda/B\cos\theta$, [15] where D_{hkl}, λ, B, and θ are the volume-averaged particle diameter, X-ray wavelength, full width at half maximum (FWHM), and diffraction angle, respectively. The results are shown in Fig 5.

Fig. 5

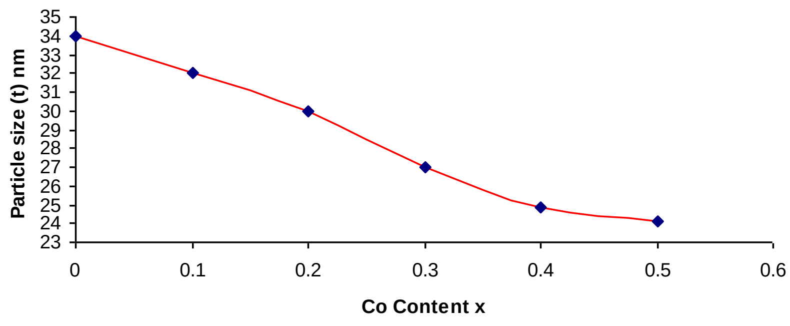

The present results depict that the increasing concentration of cobalt Co^{2+} decreases the particle size. This may be due to migration of small number of Co^{2+} ions in the midst of Co^{3+} ions in B-sites. This observation is similar to that of Caltun et al. [16] for Co-Mn ferrite. The hopping length for tetrahedral A-site (L_A) and octahedral B-sites (L_B) are calculated using the values of lattice constant. The variation of hopping lengths with Cr content x is shown in Fig. 6a & 6b.

Fig. 6 a

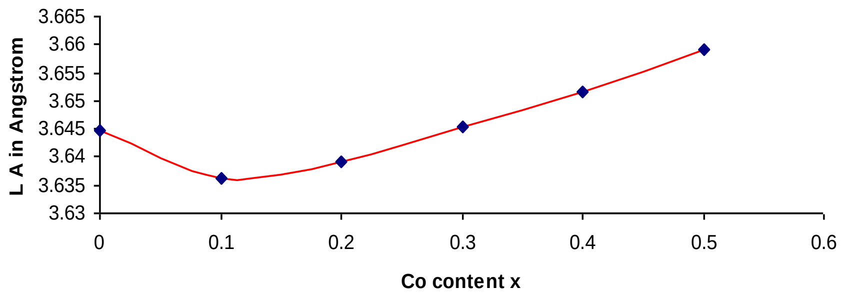

It is observed from Fig. 6a & 6b that the distance between the magnetic ions (hopping length) increases as Co content *x* increases. This could be related to the larger radius of Co^{2+} ions as compared to Cu^{3+} ions and the site occupancy of the constituent ions in the present ferrite system.

Table 1

Tetrahedral bond (d_{Ax}), Octahedral bond (d_{Bx}), Tetra edge (d_{AxE}) and octaedge (Shared d_{BXE} and unshared d_{BXEU}). The error estimates is (± 0.002 Å).

x	d_{AX} (Å)	d_{BX} (Å)	Tetra edge (Å)	Octa edge (Å)	
			d_{AXE}	d_{BXE}	d_{BXEU}
0	1.907	2.054	3.113	2.831	2.981
0.1	1.904	2.050	3.106	2.820	2.973
0.2	1.905	2.051	3.109	2.825	2.974
0.3	1.907	2.053	3.113	2.828	2.978
0.4	1.909	2.055	3.116	2.831	2.982
0.5	1.911	2.057	3.121	2.835	2.985

3.2 Cation distribution:

The cation distribution in the present system was obtained from the analysis of X-ray diffraction patterns. In this method the observed intensity ratios were compared with the calculated intensity ratios. In the present study Bertaut method [18] is used to determine the cation distribution. This method selects a few pairs of reflections according to the expression

$$\frac{I_{hkl}^{Obs.}}{I_{h'k'l'}^{Obs.}} \propto \frac{I_{hkl}^{Calc.}}{I_{h'k'l'}^{Calc.}} \qquad (1)$$

where, $I_{hkl}^{Obs.}$ and $I_{hkl}^{Calc.}$ are the observed and calculated intensities for reflection (hkl), respectively. The atomic scattering factor for various ions was taken from the literature [19]. It should be added that the calculated integrated intensities are valid at 0°K. Since the observed values are obtained at room temperature, a suitable correction is in principle necessary for the precise comparison.

The variation of mean ionic radius of the A-site (r_A) and of the B-site (r_B) with Co is shown in Fig. 7a & 7b.

Fig. 7a

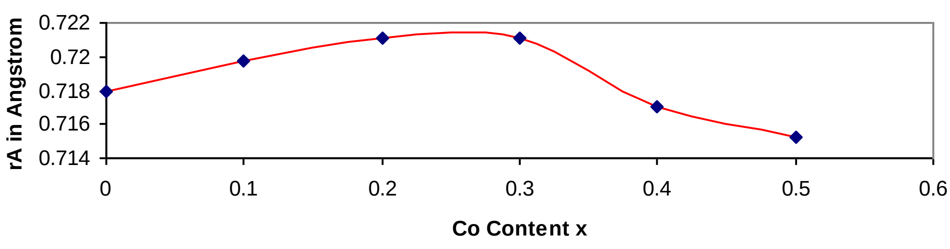

Fig. 7b

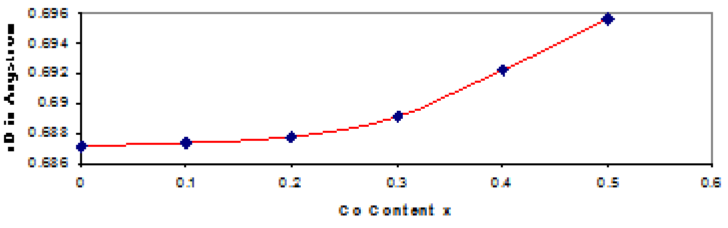

The r_A increases up to $x \le 0.3$, this is due the increase in migration of larger Cu^{2+} (0.72 Å) ions from B site to A site which replaces smaller Fe^{3+} (0.67 Å) ions at B site.

$$r_A = \left(u - \frac{1}{4}\right)a\sqrt{3} - R_0 \qquad (5)$$

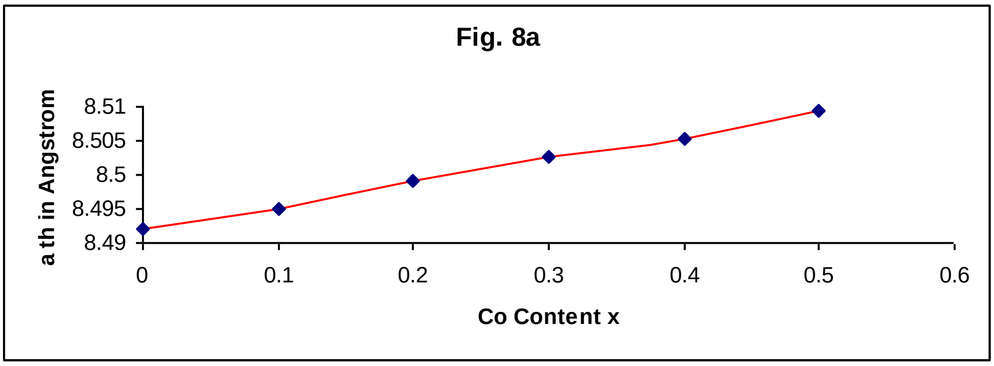

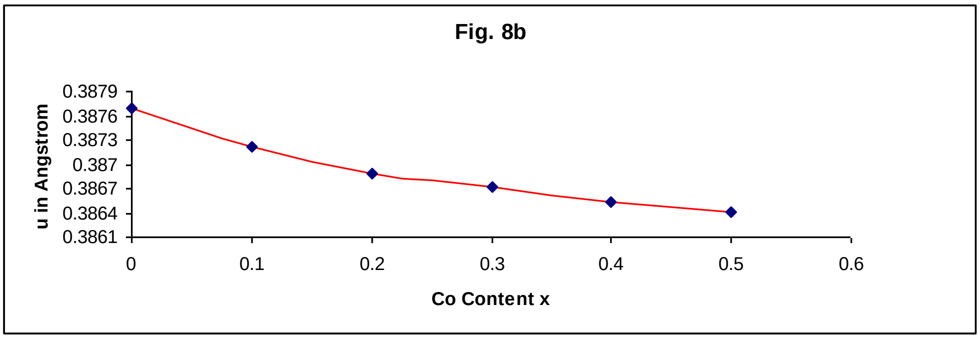

Fig. 8a & 8b shows decreasing value of oxygen positional parameter 'u' from 0.387 to 0.386 (Å). In most oxide spinels the oxygen ions are apparently larger then the metallic ions. Taking origin at one of the octahedral site, the oxygen positional parameter has a value equal to 0.250 instead of 0.375 (for ideal fcc packing) as conventionally reported by many authors [25,26]. The *u* has a value 0.375 when the origin is chosen on the tetrahedral sites but the structure is acentric and the structure factor calculation is less direct [27]. For pure magnetite *u*=0.382 and even higher values like 0.384 for Ga-substituted ferrites [28] and *u*=0.390 for Cd-Zn [29] using XRD techniques are reported.

3.3 Magnetic properties:

Room temperature hysteresis loops with the field of 7 kOe, for all the samples are shown in Fig. 9.

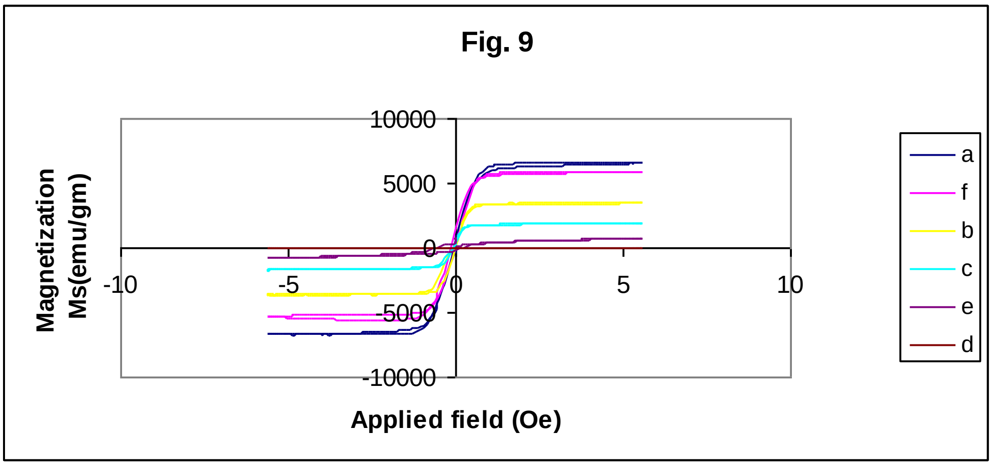

IV. Conclusions

The main conclusions that may be derived from the obtained results are:

- Copper nitrate, Cobalt nitrate, zinc nitrate and interacted with ferric nitrate at temperatures starting from 600 ^{0}C yielding $Cu_{0.61-x}Co_xZn_{0.39}Fe_2O_4$.
- Samples have some significance in magnetic recording media.

References

[1]. H.H. Hamdeh, J.C. Ho, S.A. Oliver, R.J. Willey, G. Oliver, G. Busca, J. Appl. Phys. 81 (1997) 1851.
[2]. M. Yokoyama, A. Nakamura, T. Sato, K. Haneda, J. Magn. Soc. Jpn. 22 (Suppl. S1) (1998) 243.
[3]. G. Nicoara, D. Fratiloiu, M. Nogues, J.L. Dormann, F. Vasiliu, Mater. Sci. Forum 235–238 (1997) 145.
[4]. E. Kester, B. Gillot, C. Villette, Ph. Tailhades, A. Rousset, Thermodynam. Acta 297 (1997) 71.
[5]. R. Kulkarni, V.U. Patil, J. Mater. Sci. 17 (1982) 843.
[6]. N.S. Satyamurthy, M.G. Natera, S.I. Youssef, R.J. Begum, C.M. Srivastava, Phys. Rev. 181 (2) (1969) 969.
[7]. Muhammad Ajmal, Asghari Maqsood, J. Alloys Compd. 460 (2008) 54
[8]. Sagar E. Shirsath, B. G. Toksha, K. M. Jadhav, Mater. Chem. Phys. 117 (2009) 163.
[9]. S. M. Patange, Sagar E. Shirsath, B. G. Toksha, S. S. Jadhav and K. M. Jadhav, J. Appl. Phys. 106 (2009) 1.
[10]. B.G. Toksha, Sagar E. Shirsath, S.M. Patange, K.M. Jadhav, Solid State Commun. 147(2008) 479.
[11]. Selvan RK, Augusin CO, Berchmans LJ, Saraswathi R. Mater Res Bull 2003;38:41.
[12]. C. G. Whinfrey, D. W. Eckort, A. Tayber, J. Am. Chem. Soc. 82 (1960) 2695
[13]. N. Izaoumen, M. Cherrab, K. Rissouli, K. Benkhouja, K. Jaafari and M. Fahad, J. Phys. IV France 123 (2005) 291
[14]. R.C. Kambale, P.A. Shaikh, S.S. Kamble, Y.D. Kolekar, Journal of Alloys and Compounds 478 (2009) 599
[15]. V. G. Patil, Sagar E. Shirsath, S. D. More, S. J. Shukla, K. M. Jadhav, J. Alloys. Compd. (2009) In press.
[16]. Ovidiu Caltun, G.S.N. Rao, K.H. Rao, B.P. Rao, Ioan Dumitru, Choung-Oh Kim, CheolGi Kim, J. Magn. Magn. Mater. 316 (2007) e618–e620.
[17]. S. M. Patange, Sagar E. Shirsath, B. G. Toksha, S. S. Jadhav, S. J. Shukla, K. M. Jadhav, Appl. Phys. A: 95 (2009) 429.
[18]. L. Weil, E. F. Bertaut, L. Bochirol. J. Phys. Radium, 11 (1950) 208.
[19]. B.D. Cullity, Introduction to Magnetic Materials, Addison-Wesley, MA, 1972, p. 141.
[20]. J.W. Vrewey, E.L. Heilmann, J. Chem. Phys. 15 (4) (1947) 174–180.
[21]. T. Abbas, Y. Khan, M. Ahmad, S. Anwar, Solid State Comm. 82 (9) (1992) 701–703.
[22]. G. Fagherazzi, F. Garbassi, J. Appl. Crystallogr. 5 (1977) 18.
[23]. C.O. Arean, J.L.R. Blanco, J.M.R. Gonzalez, M.C.T. Fernandez, J. Mater. Sci. Letts. 9 (1990) 229
[24]. C.O. Arean, E.G. Diaz, J.M.R. Gonzalez, M.A.V. Garcia, Solid State Comm. 77 (1988) 275.
[25]. J. Smit, H.P.T. Wijn, Ferrites, Wiley, New York, 1959.
[26]. S.I. Patil and Raka V. Dabhade, IEEE Trans. Mang. 30 (1994) 4915
[27]. L. Néel. C. R. Acad. Sci. Paris 230 (1950) 375.
[28]. O. Caltun, H. Chirac, Lupu., I. Dumitru., P.B. Rao, J. Opto. Adv. Mater. 9 (2007) 1158.
[29]. Y. Yafet, C. Kittel, Phys. Rev. 90 (1952) 295.

D. D. Birajdar. "Crystallographic and Magnetic Properties with Increasing Co2+ In Cu0.60-Xcoxzn0.40Fe2O4 (0 ≤ X ≤ 0.5) Nanoferrites." IOSR Journal of Applied Physics (IOSR-JAP) , vol. 10, no. 6, 2018, pp. 58-63